Pressure-induced superconductivity in GeAs

Lixue Liu,[1] Viktor V. Struzhkin,[2,3,*] and Jianjun Ying[1,†]

[1]*Hefei National Laboratory for Physical Sciences at Microscale and Department of Physics, University of Science and Technology of China, Hefei, Anhui 230026, China*

[2]*Center for High Pressure Science and Technology Advanced Research, Shanghai, China*

[3]*Geophysical Laboratory, Carnegie Institution of Washington, Washington, DC 20015, USA*

(Received 22 October 2019; published 27 December 2019)

We performed high-pressure Raman and resistance measurements on a two-dimensional monoclinic semiconductor GeAs. We discovered a superconductivity that emerges after the insulator-metal transition above 10 GPa, which is related to the structural transition. Our results indicate that the semiconducting monoclinic phase and rocksalt structure phase coexist above 10 GPa and structural transformation to the rocksalt phase is completed above 17∼18 GPa. The maximum superconducting transition temperature T_c is about 8 K close to the structural transition boundary, and the T_c is gradually decreasing at higher pressures. Upon pressure release, the nonpolar rocksalt structure transforms to a polar tetragonal superconducting phase. Our first-principles calculations indicate that the relatively high T_c in the rocksalt phase is mainly due to the enhancement of the electron-phonon coupling. These results show that superconductivity in this material strongly depends on its structure, achieving maximum T_c in a higher-symmetry phase.

DOI: 10.1103/PhysRevB.100.214516

I. INTRODUCTION

Since the first successful exfoliation of graphite into monolayer or few-layers sheets made possible due to weak coupling between the layers, the two-dimensional materials have attracted tremendous interest due to their novel electronic and optical properties [1]. Plenty of novel layered materials were studied as potential two-dimensional materials. It is known that silicon and germanium phosphides and arsenides can crystallize in orthorhombic or monoclinic layered structures [2,3], which could also have a potential to be two-dimensional materials. However, very few studies were performed on this type of materials, possibly due to their complex low-symmetry structures. Although some theoretical calculations indicate that this type of material may be used in optical devices and thermoelectric application [4,5], their physical properties were not fully explored and more experiments are needed to explore their emergent physical properties.

The monoclinic semiconductor GeAs with a band gap around 1 eV [6] shows highly anisotropic optical and electronic properties [7,8], and is characterized as highly anisotropic van der Waals thermoelectric material at ambient pressure [9], which may have future applications in functional electronics, optoelectronics, and in thermoelectric devices. Optimization and tuning of its structure may enhance the electronic, optoelectronic, and thermoelectric properties, as well as lead to novel physical properties. High pressure is one of the effective methods to provide such tuning of the physical properties of the materials. By applying high pressure, many new superconductors were found, especially some high-T_c superconductors such as H_3S [10], which initiated great progress in the field of superconductivity. Early high-pressure work indicates that GeAs transforms to the simple rocksalt structure above 13 GPa accompanied by an insulator-metal transition [11]. Here, we combined the high-pressure Raman and resistance measurements on this layered material, and we found that the monoclinic and rocksalt structures coexist in a wide pressure range. More interestingly, the superconductivity emerges in the metallic rocksalt phase. The maximum measured T_c is around 8 K, the highest T_c observed in such binary materials. On pressure release, the cubic phase transforms to a superconducting tetragonal phase. Our first-principles calculations indicate that the relatively high T_c in the rocksalt phase is mainly due to the enhancement of the electron-phonon coupling.

II. METHODS

We conducted the electrical transport measurements on a GeAs single crystal under pressure by using the miniature diamond anvil cell [12]. High-quality single crystals of GeAs were grown as previously reported [11]. Diamond anvils with 300 μm culet and c-BN gasket with sample chambers of diameter 110 μm were used. An GeAs single crystal was cut with the dimensions of $60\times60\times10$ μm^3. NaCl was used as a pressure-transmitting medium. Resistivity was measured using a Quantum Design Physical Properties Measurement System. Diamond anvil with 300 μm culet was used for the high-pressure Raman measurements with incident laser wavelength of 660 nm. Neon was loaded as the pressure transmitting medium. Pressure was calibrated by using ruby fluorescence shift at room temperature for both the transport and Raman measurements.

*viktor.struzhkin@hpstar.ac.cn
†yingjj@ustc.edu.cn

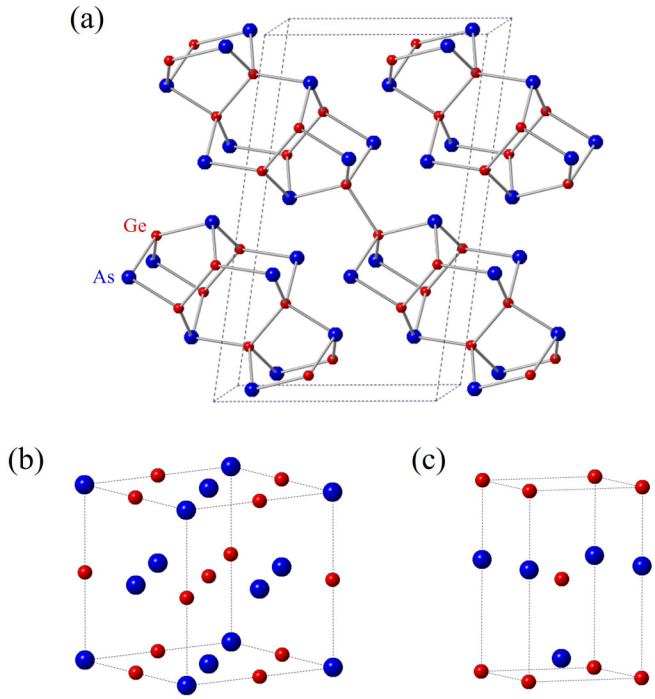

FIG. 1. (a) The layered monoclinic crystal structure of GeAs. (b) The rocksalt structure of GeAs at high pressure. (c) The polar tetragonal structure of GeAs decompressed from high pressure.

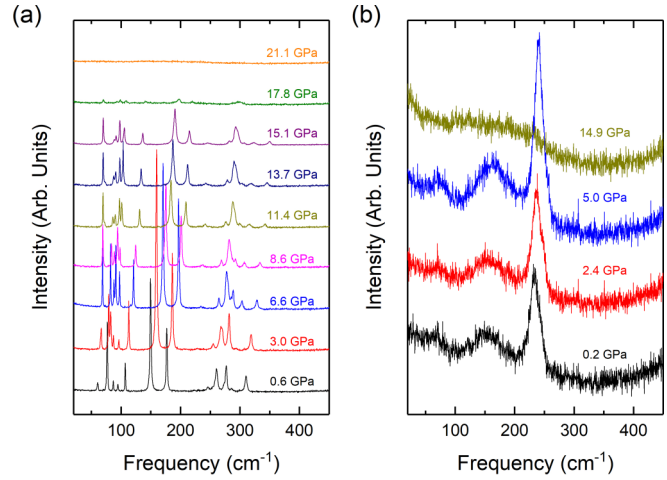

FIG. 2. (a) Raman spectra of GeAs at several pressures. The monoclinic structure has many Raman modes; all the Raman modes disappear above 18 GPa, which indicates that the monoclinic phase transforms completely to the rocksalt structure. (b) The Raman spectra of GeAs during decompression cycle. The Raman spectra indicate that the phase sequence during compression-decompression process is irreversible. The spectra show several broad peaks at decompression, which may related to the tetragonal phase.

Our electronic structure calculations were performed within density functional theory (DFT) using the Vienna *ab initio* simulation package (VASP) [13] with projector-augmented-wave potentials [14,15] and the Perdew-Burke-Ernzerhof version of generalized gradient approximation for exchange-correlation functional [16]. The default plane-wave cutoff energy of 250 eV was used in two phases. The Monkhorst-Pack scheme was used for Brillouin zone sampling [17]. The structures were fully relaxed without any symmetry constraints until the force on each atom was smaller than 0.01 eV/Å and the electronic self-consistent calculation was stopped at the energy convergence less than 1.0×10^{-6} eV. The phonon modes were calculated by QUANTUM ESPRESSO program [18] using the PAW potentials. For this calculation, we employed a $4\times4\times4$ q mesh and a $12\times12\times12$ k mesh. To interpolate the e-ph coupling, the Brillouin zone of both phases was initially sampled by a dense $24\times24\times24$ k mesh. The superconducting T_c was then estimated using the Migdal-Eliashberg method with several values of Gaussian broadening for the evaluation of the related integrals.

III. RESULTS AND DISCUSSION

The two-dimensional GeAs under ambient pressure forms monoclinic structure as shown in Fig. 1(a). GeAs is isostructural to GaTe and SiAs [3,19] with the space group $C2/m$ (No. 12). The GeAs crystallizes in a layered structure; within each layer Ge-Ge dumbbells are octahedrally coordinated by arsenic atoms as shown in Fig. 1(a). Previous x-ray diffraction studies indicate a structural transition around 13 GPa: the monoclinic structure transforms to the rocksalt structure. After decompression from high pressure, the structural change occurs to a tetragonal phase with the space group $I4mm$ [11]. This tetragonal phase lacks inversion symmetry with all the As ions equally shifted towards their adjacent Ge ions along the c axis, thus inducing a net dipolar electric moment along the c axis. This polar tetragonal structure can also be synthesized at high temperature around 6.5 GPa [20]. Figures 1(b) and 1(c) show the high-pressure rocksalt structure and decompressed tetragonal structure, respectively.

In order to check the phase transitions under pressure, we performed high-pressure Raman measurements. The Raman spectra at low-pressure exhibit many peaks due to the low symmetry of the monoclinic structure as shown in Fig. 2(a), which is consistent with previous measurements [7,8]. On pressure increase, all the peaks shift to higher frequency. When the pressure is above 17∼18 GPa, all the peaks disappear, which indicates that the sample transformation to the rocksalt structure is complete. During the decompression process, new broad peaks appear when the pressure is decreased to 5 GPa as shown in Fig. 2(b). This indicates that the nonpolar rocksalt structure transforms to the polar tetragonal structure at low pressure. Our Raman results are consistent with the phase transitions proposed from the previous XRD measurements.

In order to search for the new physical properties under pressure, we performed high-pressure resistance measurement on a monoclinic GeAs single crystal. GeAs exhibits the insulating behavior at low pressure similar with its ambient pressure behavior [21]. By increasing the pressure, the insulating behavior is suppressed gradually and an insulator-metal transition occurs above 10 GPa. More interestingly, the resistance shows a sudden drop at low temperature when the system evolves to the metallic state. Such sharp decrease of the resistance is due to the superconducting

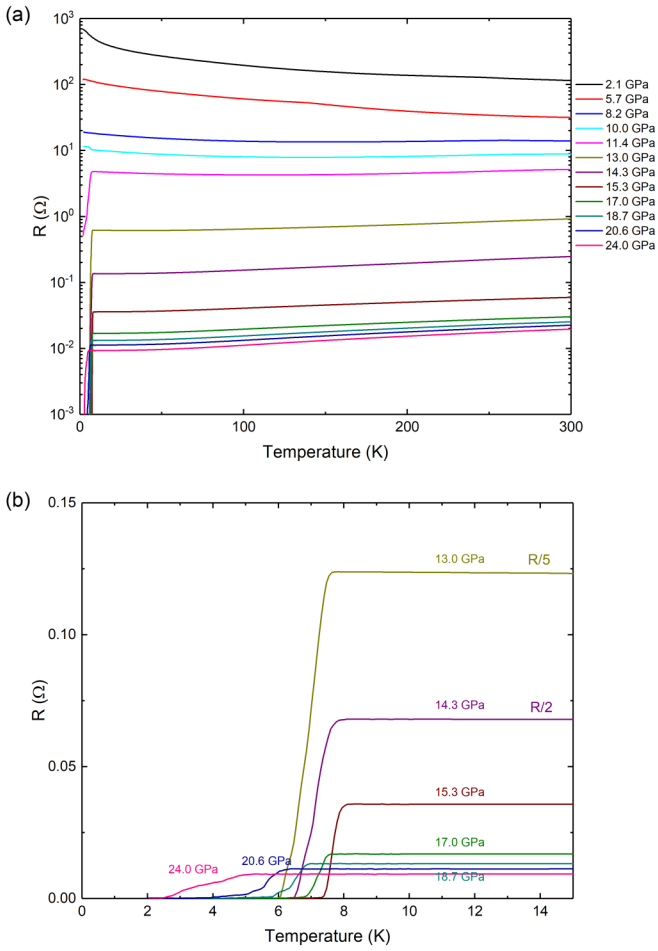

FIG. 3. (a) The temperature dependence of the resistance of GeAs at various pressures. Insulator-metal transition appears around 10 GPa, followed by the superconductivity. (b) The resistance around the superconducting transition temperature (expanded). The T_c increases with increasing pressure and the maximum $T_c \sim 8$ K is reached around 15.3 GPa. The resistance data at 13 and 14.3 GPa were divided by the factor 5 and 2, respectively.

transition, and zero resistance is reached above 13 GPa as shown in Fig. 3(b). The maximum $T_c \sim 8$ K occurs around 15.3 GPa, close to the structural transition boundary. Above 15.3 GPa, the T_c is suppressed gradually, and the superconducting transition becomes much broader with increasing pressure.

We also applied magnetic field to suppress the superconducting transition. The temperature dependences of the resistivity of GeAs at pressure of 15.3 GPa with various applied magnetic fields are shown in the inset of Fig. 4. From this data we can obtain the upper critical field (H_{c2}). The H_{c2} shows a linear dependence with respect to the T_c as shown in Fig. 4. Within the weak-coupling BCS theory, the upper critical field at $T = 0$ K can be determined by the Werthamer-Helfand-Hohenberg (WHH) equation [22] $H_{c2}(0) = 0.693[-(dH_{c2}/dT)]_{T_c}T_c$. We can deduce that $H_{c2}(0) \sim 0.65$ T.

By combining the high-pressure resistance and Raman results, we can map out the phase diagram of GeAs as shown

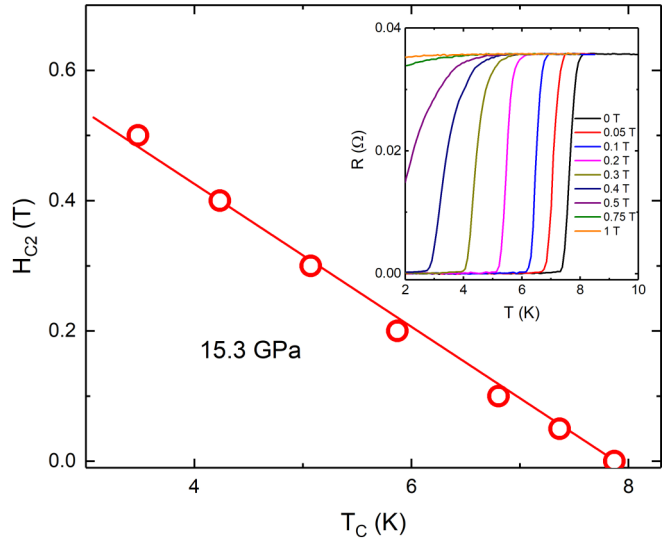

FIG. 4. The upper critical field H_{c2} at 15.3 GPa. The inset shows the temperature dependence of the resistivity of GeAs at 15.3 GPa at several applied magnetic fields. The T_c was determined from the 90% resistivity transition.

in Fig. 5. The resistivity at 300 K shows a rapid decrease above 10 GPa, which is related to the insulator-metal transition. Such a rapid decrease of the resistivity is leveled of above $17 \sim 18$ GPa, at which pressures the structure is transformed completely to the rocksalt structure, as follows from the Raman measurements. Since previous XRD measurements indicate that the structural transition occurs at around 13 GPa, we attributed the insulator-metal transition to this structural transition. We can see that the structural transition starts around 10 GPa and the low-pressure phase persists up to 17∼18 GPa. Thus, the monoclinic and rocksalt phases coexist in a large pressure range. Although we used the nearly hydrostatic Ne pressure medium for the Raman measurements, and

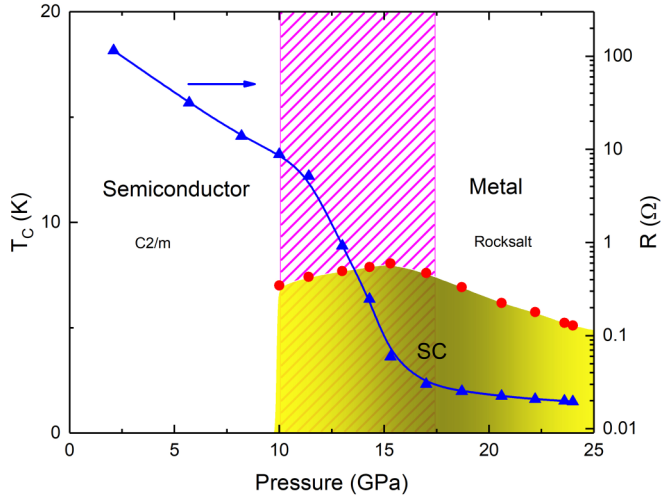

FIG. 5. The phase diagram of GeAs at high pressure. The dome-like T_c appears after the insulator-metal transition. The pressure dependence of the resistivity at 300 K indicates that the monoclinic and rocksalt structures coexists between 10–17.5 GPa (dashed area), which is consistent with the Raman measurements.

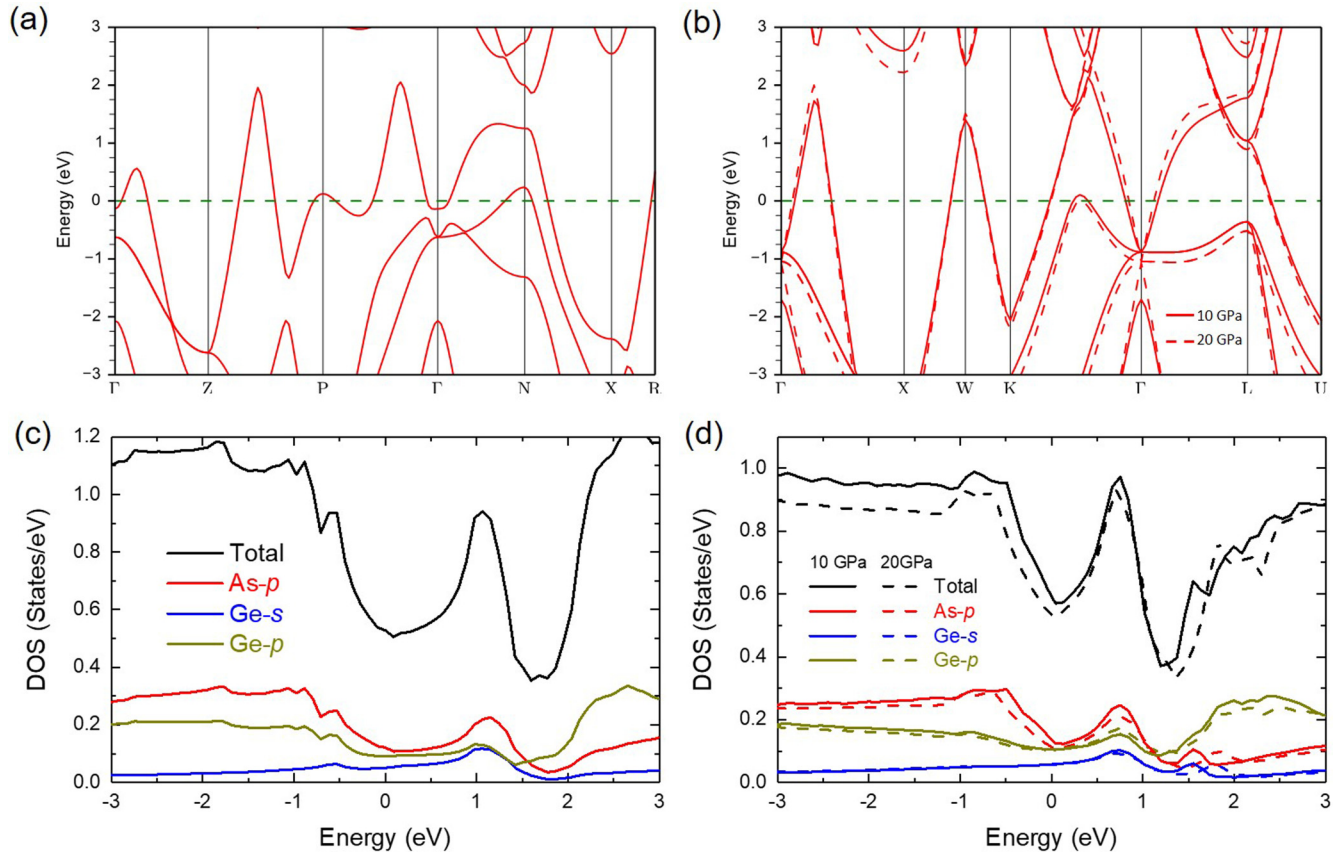

FIG. 6. (a) The band structure of the polar tetragonal phase at ambient pressure and (b) of the nonpolar rocksalt phase at 10 and 20 GPa. The calculated density of electronic states for (c) tetragonal and (d) rocksalt phases. The solid and dashed lines represent calculated results at 10 and 20 GPa, respectively, for the rocksalt phase.

solid NaCl pressure medium for the resistivity measurements, the results are consistent with each other. Both of the pressure media provide good hydrostatic environment in our experiments evidenced by the ruby fluorescence spectra shown in the Supplemental Material [23]. The small nonhydrostatic effects by using different pressure media do not significantly affect the phase transition in this sample, and the large coexistence region is most likely not related to the nonhydrostatic effects.

During the pressure release, the nonpolar rocksalt phase does not turn back to the original monoclinic phase, but changes instead to a polar tetragonal phase as evidenced by our Raman measurements and previous XRD measurements. However, the T_c of the polar tetragonal phase is only 3∼3.5 K [20], which is much lower than the T_c in the rocksalt phase. In order to figure out the origin of the superconductivity in both phases, we compared the electronic band structure and projected electronic density of states (DOS) for the polar tetragonal phase at ambient pressure and for nonpolar cubic phase at 10 and 20 GPa as shown in Fig. 6. Several bands cross the Fermi level confirming the metallic nature of both phases. The densities of electronic states for both phases show remarkable similarity. At higher pressure, the total DOS of the rocksalt phase decreases mainly due to the reduction of the DOS for As p orbitals, thus the T_c would also decrease in agreement with our experimental observations.

The phonon band structure and phonon density of states were calculated to determine the dynamic stability of the observed phases as shown in Figs. 7(a) and 7(b) for the polar tetragonal phase at ambient pressure and for the nonpolar cubic phase at 10 and 20 GPa, respectively. The absence of imaginary frequency modes in the entire Brillouin zone indicates the dynamic stability of these structures. The electron-phonon coupling parameter λ, and the Eliashberg phonon spectral function $\alpha^2F(\omega)$ were calculated to obtain theoretical predictions for the superconductivity of both polar and nonpolar phases. The right panel of Figs. 7(a) and 7(b) shows the frequency dependence of λ and $\alpha^2F(\omega)$ for the polar tetragonal phase at ambient pressure and for the nonpolar cubic phase at 10 and 20 GPa, respectively. The calculated λ for the polar tetragonal phase is 0.52, which is smaller than the $\lambda = 0.65$ for the rocksalt structure at 10 GPa. The superconducting transition temperature (T_c) can be estimated by the modified (by Allen and Dynes) McMillan's equation [24,25] $T_c = \omega_{\log}/1.2 \exp[-1.04(1+\lambda)/\{P\lambda - \mu^*(1+0.62\lambda)\}]$ using $\mu^* = 0.1$, the calculated $\omega_{\log}$ is 180.7 and 195.4 K, and the resultant T_c is 2.6 and 5.6 K for the polar phase at ambient pressure and for the nonpolar phase at 10 GPa, respectively. The calculated T_c values are in reasonable agreement with the experimental values. With the pressure increase to 20 GPa in the nonpolar rocksalt phase, the λ decreases to 0.51 and $\omega_{\log}$ increases to 267.3 K, thus the calculated T_c decreases to 3.5 K in agreement with the experiment.

Our results indicate that the nonpolar cubic GeAs shows the maximum T_c above 8 K, which is the highest

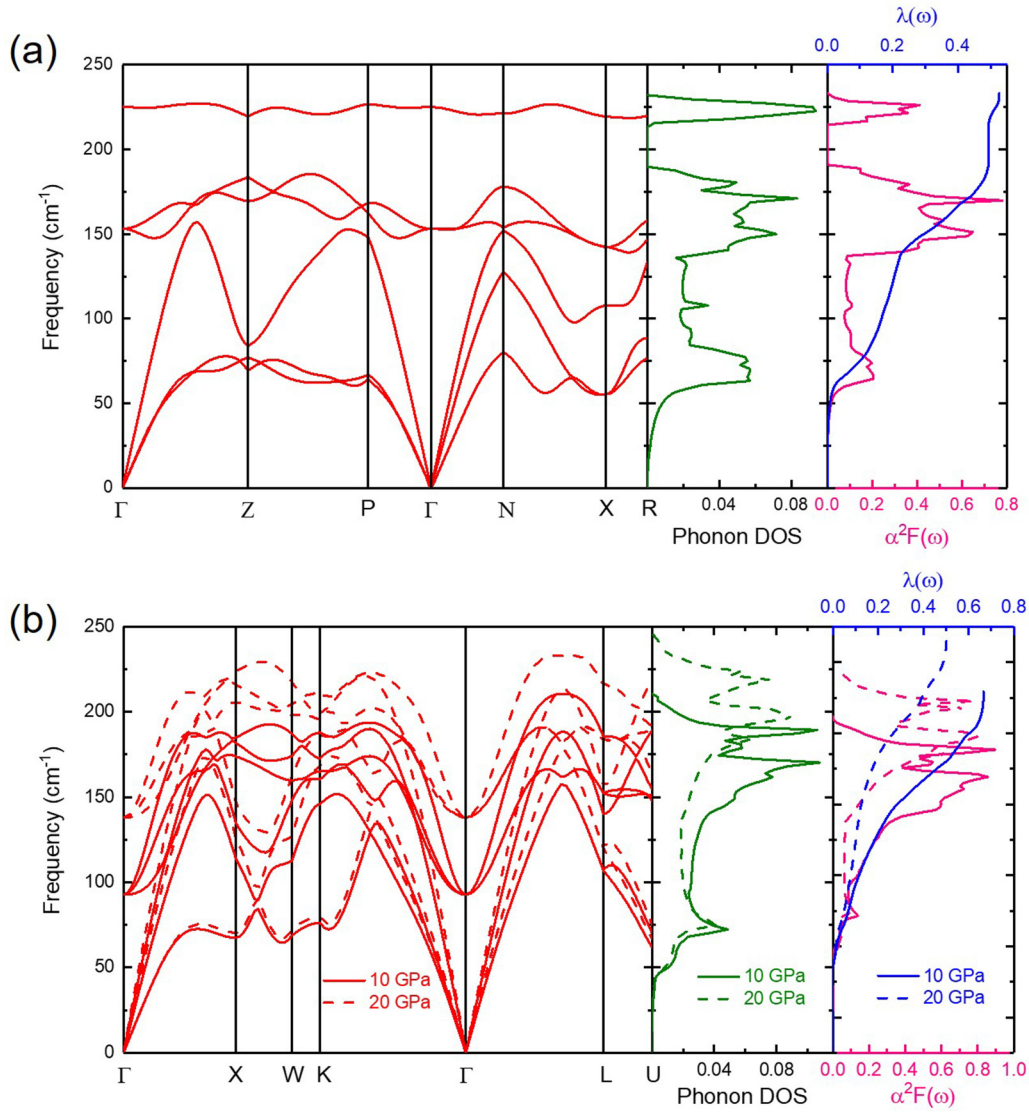

FIG. 7. (a) The phonon energy dispersion curves, the phonon density of states, frequency dependence of λ and $\alpha^2F(\omega)$ for the polar tetragonal phase at ambient pressure; (b) the same for the nonpolar cubic phase at 10 and 20 GPa. The solid and dashed lines represent the calculated results at 10 and 20 GPa, respectively, for the rocksalt phase.

transition temperature in this type of material. Since the Raman scattering is a much more sensitive method to detect the phase transitions at hand, our experimental results indicate that the monoclinic and rocksalt structures coexist in a wide pressure range. Insulator-metal transition is concomitant with the structural transition as evidenced by the transport measurements. After decompression, the system changes to a polar tetragonal structure and superconductivity is suppressed to $3 \sim 3.5$ K [20]. These results indicate that the superconductivity correlates strongly with the structure of the material. Ga-doped cubic Ge shows superconductivity at 0.5 K [26] at ambient pressure. The T_c can be enhanced to 5 K under high pressure [27], however, in this case the structure changes to a β-Sn structure, which is completely different in comparison to the rocksalt structure of GeAs. The maximum superconducting T_c in compressed As is below 2.5 K [28] within the simple cubic structure, which is quite similar to the rocksalt phase of GeAs. The rocksalt structure of GeAs can be treated so as the half of the As atoms were substituted by the Ge atoms in the simple cubic As phase. Compared to the cubic phases of elements (Ge and As), the T_c is greatly enhanced in the rocksalt structure of GeAs, which may be possibly due to the enhancement of the average phonon frequency and/or the electron-phonon coupling. The pressure-mediated polar-nonpolar structural transition was also observed in SnP [29], but the maximum T_c in SnP system is only 3.4 K, which is much lower than the maximum T_c in the GeAs. Our DFT calculation results indicate that the electron-phonon coupling parameter λ may be the main source of the T_c enhancement in the GeAs material having the rocksalt structure.

IV. CONCLUSIONS

In conclusion, we observed the superconductivity in the rocksalt GeAs phase with the maximum T_c up to 8 K,

which is the highest T_c reported in this type of material. The monoclinic phase coexists with the rocksalt phase in a wide pressure range. The sample transforms to the polar superconducting tetragonal phase after decompression to low pressures. Our results constrain the high-pressure phase diagram and superconducting properties in this binary GeAs material.

ACKNOWLEDGMENTS

This work was supported by the Fundamental Research Funds for the Central Universities (WK2030020031). J.Y. acknowledges support by the CAS Pioneer Hundred Talents Program. V.V.S. acknowledges support from the Thousand Talent Program by the State Council of the People's Republic of China.

[1] Q. H. Wang, K. Kalantar-Zadeh, A. Kis, J. N. Coleman, and M. S. Strano, Nat. Nanotechnol. **7**, 699 (2012).
[2] T. Wadsten, Chem. Scr. **8**, 63 (1975).
[3] T. Wadsten, Acta Chem. Scand. **21**, 593 (1967).
[4] S. Zhang, S. Guo, Y. Huang, Z. Zhu, B. Cai, M. Xie, W. Zhou, and H. Zeng, 2D Mater. **4**, 015030 (2017).
[5] T. Zhao, Y. Sun, Z. Shuai, and D. Wang, Chem. Mater. **29**, 6261 (2017).
[6] J. W. Rau and C. R. Kannewurf, Phys. Rev. B **3**, 2581 (1971).
[7] J. Guo, Y. Liu, Y. Ma, E. Zhu, S. Lee, Z. Lu, Z. Zhao, C. Xu, S. Lee, H. Wu, K. Kovnir, Y. Huang, and X. Duan, Adv. Mater. **30**, 1705934 (2018).
[8] S. Yang, Y. Yang, M. Wu, C. Hu, W. Shen, Y. Gong, L. Huang, C. Jiang, Y. Zhang, and P. M. Ajayan, Adv. Funct. Mater. **28**, 1707379 (2018).
[9] K. Lee, S. Kamali, T. Ericsson, M. Bellard, and K. Kovnir, Chem. Mater. **28**, 2776 (2016).
[10] A. P. Drozdov, M. I. Eremets, I. A. Troyan, V. Ksenofontov, and S. I. Shylin, Nature (London) **525**, 73 (2015).
[11] U. Schwarz and K. Syassen, High Press. Res. **9**, 148 (1992).
[12] A. G. Gavriliuk, A. A. Mironovich, and V. V. Struzhkin, Rev. Sci. Instrum. **80**, 043906 (2009).
[13] G. Kresse and J. Furthmüller, Phys. Rev. B **54**, 11169 (1996).
[14] P. E. Blöchl, Phys. Rev. B **50**, 17953 (1994).
[15] G. Kresse and D. Joubert, Phys. Rev. B **59**, 1758 (1999).
[16] J. P. Perdew, K. Burke, and M. Ernzerhof, Phys. Rev. Lett. **77**, 3865 (1996).
[17] H. J. Monkhorst and J. D. Pack, Phys. Rev. B **13**, 5188 (1976).
[18] P. Giannozzi, S. Baroni, N. Bonini, M. Calandra, R. Car, C. Cavazzoni, D. Ceresoli, G. Chiarotti, M. Cococcioni, I. Dabo *et al.*, J. Phys.: Condens. Matter **21**, 395502 (2009).
[19] T. Wadsten, Acta Chem. Scand. **19**, 1232 (1965).
[20] P. C. Donohue and H. S. Young, J. Solid State Chem. **1**, 143 (1970).
[21] C. Barreteau, B. Michon, C. Besnard, and E. Giannini, J. Cryst. Growth **443**, 75 (2016).
[22] N. R. Werthamer, E. Helfand, and P. C. Hohenberg, Phys. Rev. **147**, 295 (1966).
[23] See Supplemental Material at http://link.aps.org/supplemental/10.1103/PhysRevB.100.214516 for details of the fluorescence spectra of ruby by using neon and NaCl as pressure media.
[24] W. L. McMillan, Phys. Rev. **167**, 331 (1968).
[25] P. B. Allen and R. C. Dynes, Phys. Rev. B **12**, 905 (1975).
[26] T. Herrmannsdörfer, V. Heera, O. Ignatchik, M. Uhlarz, A. Mücklich, M. Posselt, H. Reuther, B. Schmidt, K.-H. Heinig, W. Skorupa *et al.*, Phys. Rev. Lett. **102**, 217003 (2009).
[27] W. Buckel and J. Wittig, Phys. Lett. **17**, 187 (1965).
[28] A. L. Chen, S. P. Lewis, Z. Su, P. Y. Yu, and M. L. Cohen, Phys. Rev. B **46**, 5523 (1992).
[29] M. Kamitani, M. S. Bahramy, T. Nakajima, C. Terakura, D. Hashizume, T. Arima, and Y. Tokura, Phys. Rev. Lett. **119**, 207001 (2017).